E 11907

# Experimental Study of Unsupported Nonane Fuel Droplet Combustion in Microgravity

B.J. Callahan, C.T. Avedisian, D.E. Hertzog and J.W. Berkery
Sibley School of Mechanical and Aerospace Engineering
Cornell University
Ithaca, New York 14853-7501

## 1. Introduction

Soot formation in droplet flames is the basic component of the particulate emission process that occurs in spray combustion. The complexity of soot formation motivates a one-dimensional transport condition which has obvious advantages in modeling. Recent models of spherically symmetric droplet combustion have made this assumption when incorporating such aspects as detailed chemistry [1-3] and radiation [4]. Interestingly, spherical symmetry does not necessarily restrict the results because it has been observed that the properties of carbon formed in flames are not strongly affected by the nature of the fuel or flaming configuration [5,6]. What is affected, however, are the forces acting on the soot aggregates and where they are trapped by a balance of drag and thermophoretic forces. The distribution of these forces depends on the transport conditions of the flame.

Prior studies of spherical droplet flames as reviewed in reference 7 have examined the droplet burning history of alkanes, alcohols and aromatics. Data are typically the evolution of droplet, flame, extinction, and soot shell diameters. These data are only now just beginning to find their way into comprehensive numerical models of droplet combustion to test proposed oxidation schemes for fuels such as methanol [3] and heptane [2,4].

In the present study, we report new measurements on the burning history of unsupported nonane droplets in a convection-free environment to promote spherical symmetry. The far-field gas is atmospheric pressure air at room temperature. The evolution of droplet diameter was measured using high speed cine photography of a spark-ignited, droplet within a confined volume in a drop tower. The initial droplet diameters varied between 0.5mm and 0.6mm. The challenge of unsupported droplets is to form, deploy and ignite them with minimal disturbance, and then to keep them in the camera field of view. Because of the difficulty of this undertaking, more sophisticated diagnostics for studying soot than photographic were not used. Supporting the test droplet by a fiber fixes the droplet position but the fiber can perturb the burning process especially for a sooting fuel (Avedisian 1998).

Prior studies on heptane droplets of similar size [8,9] showed little evidence for soot formation due to the relationship between sooting and droplet diameter. For nonane droplets we expect increased sooting due to the greater number of carbon atoms. As a sooting droplet burns and its diameter decreases, proportionally less soot should form. This reduced soot, as well as the influence of soot formed earlier in the burning process which collects in a 'shell', on heat transport to the flame offers the potential for a time-varying burning rate. Such an effect was investigated and revealed in results reported here. Speculation is offered for the cause of this effect and its possible relation to soot formation.

## 2. Experiment

Unsupported droplets in microgravity were studied using a variation of a method reported in previous studies [8-11]. A fuel droplet is projected into a vertical trajectory in a chamber attached to a support package. At the apex of the droplet's trajectory, the package which houses the combustion chamber and surrounding instrumentation is released into free-fall. A short time later, the droplet is ignited by two sparks positioned on opposite sides of the droplet to counteract the impulse of the spark discharge on moving the droplet. The electrodes are then quickly retracted and the burning process recorded by a high speed cine camera. In the present study, the sparks are activated between 5ms and 33ms after release of the package. The smaller delay time ensures more precise positioning of the droplet between the center of the electrodes at ignition and, thus, tends to minimize the effect of the spark on droplet motion after ignition. The spark energy is about .05 J and the spark duration is 0.5ms. The droplets studied had initial diameters less than 0.6mm which are small enough to burn completely within the allowable 1.2s of the experimental free-fall time. A drag shield around the support package provided a gravity level of about $10^{-4}$ that of the Earth's normal gravity.

Several improvements were made to prior versions of this method that produced a more reliable operating procedure: 1) the timing sequences required to activate power to the spark circuit, electrodes, solenoids, and magnet was controlled by external logic circuitry interfaced with a commercial timing control box (Quantum Composers model 9318 timing box (Bozeman, Mt); 2) a continuous duty cycle electromagnet (a model CEA-400M-110M electromagnet from AEC Magnetics, Cincinnatti, Ohio) that had a more repeatable delay time was used; 2) new and more powerful electrode retraction solenoids were fabricated with

non-brushing brushes; 3) the power supply for the package was on-board the free-fall package to reduce stray signals directed to the spark circuit; and 4) droplets were propelled upward in a more vertical trajectory to reduce the horizontal velocity component at the apex.

Maintaining zero residual velocity at the apex by a vertical trajectory proved helpful for aligning the droplet between the twin ignition sparks (four electrodes) to insure symmetric impulse forces during ignition, which is the key for keeping the droplet velocity low after ignition. Unfortunately, this configuration forces the droplets prior to the experimental droplet to splash on the nozzle face, which could affect the stream. This was not a problem as long as the nozzle was flat, horizontal, and small enough such that when the liquid splashed centrally on the face, it diffused the droplet and wetted the descending walls evenly.

TIG welded, two piece, solid electrodes replaced the three-piece brushing contact electrodes used in previous studies (see Fig. 1). Eliminating the brushing contact allowed more repeatable spark energy. The positioning solenoid acted on the plunger portion which had to be ferromagnetic. The tips could not be magnetic, since that would diffuse the magnetic flux lines from the solenoid coils. The welded construction allowed electrical conduction from the leader wire to the electrode tips while employing nonmagnetic steel for the tips, and ferromagnetic steel for the plunger.

The high speed movie camera was operated at 200 frames/sec giving about 100 discrete time steps for the duration of the burn. The film images were digitized on a Microtek slide scanner at 3900 dpi, then imported into an image analysis software package. The software finds the edge of the droplet by means of categorizing the pixels according to a threshold brightness. The lighting and magnification are the same for the results presented in this study.. The resolution in the droplet diameter measurement was estimated to be $\pm 25\mu m$.

The backlighting was adjusted to show the translucent droplet and granular soot shell as a shadow but at the expense of observing the outer luminous zone of the flame. A video camera was mounted perpendicularly to the movie camera to record the droplet position along the view axis of the movie camera. A 40W halogen light mounted outside the package back-lit the droplet in the initial stages of free fall while the video camera automatic intensity gain control remained off. In this fashion, the backlight illuminated the droplet before ignition, and the camera could view the droplet and the flame after ignition using the visible flame radiation.

## 3. Results

Figure 2 shows a series of photographs of the complete burning history of a free nonane droplet from ignition to burnout. The electrodes are visible in the first two frames and are out of the field of view in later frames because of their retraction. After ignition, the droplet decreases in size while the soot shell develops as the black 'ring' structure surrounding the droplet. The shell shows reasonable sphericity except for a 'tail' that is created by a very small convection component due to the droplet's motion. This tail has been observed for other fuel types as well [7]. The outer luminous zone which could be taken as the 'flame' is faintly visible in 'c' and 'e'. In 'd' and 'e' the white 'patches' are soot aggregates that have passed through the flame and were oxidized. The last frame shows the complete burnout that was typical of our observations. Remaining is a single soot aggregate 'speck' in 'g'.

The evolution of droplet diameter is shown in fig. 3 for three data sets in coordinates that follow the classical '$d^2$ law' [12], though the variation is not consistent with that result as will be discussed below. Also shown in fig. 3 are references to fig. 2 to show where in the burning history the photographs in fig. 2 were taken. The initial diameters are essentially the same for the three data sets so that there should be no effect of droplet diameter on sooting. Several points to note about fig. 3 are the following:

1) the burning histories of the three separate runs are close to each other and show the same trends;
2) the variation of droplet diameter with time is not linear; and
3) the droplets burned to completion and left a single soot aggregate particle.

Fig. 3 shows that burning occurs progressively faster as time advances (a solid line in fig. 3 is included to better note the non-linear burning process). Soot formation can cause the burning rate to change during combustion. Early in the burning process while the droplet is still large, the incomplete combustion associated with soot formation lowers the chemical energy released by oxidation at the flame and, therefore, reduces heat transfer to the droplet. At the same time, radiative losses from the flame are larger in the early period because the flame is physically larger. As burning progresses and the droplet and flame size decrease, the droplet produces less soot per mass of fuel consumed due to the effect of droplet size on soot formation [2,8,9,13] as well as the effect of size on radiative losses from the flame [4]. The reduced sooting and radiation loss translates into a higher gasification rate. Soot that passes through, or is overtaken by, the flame will absorb heat in the high temperature zone and be carried further from the droplet because aggregates

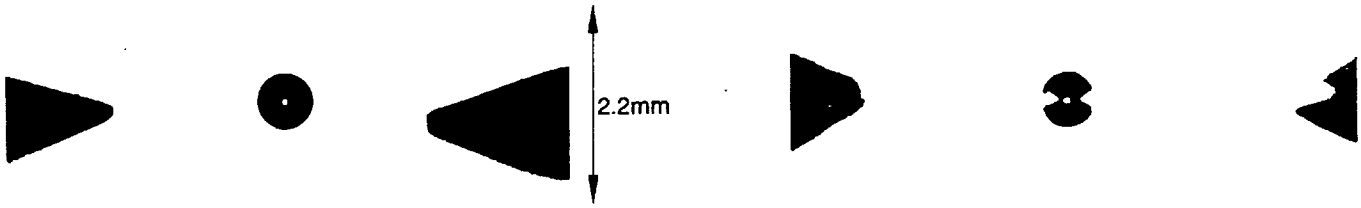


2a, -40ms

2b, 0 (ignition)

2c, 220ms

2d, 325ms

2e, 405ms

2f, 490ms

2g, 525ms

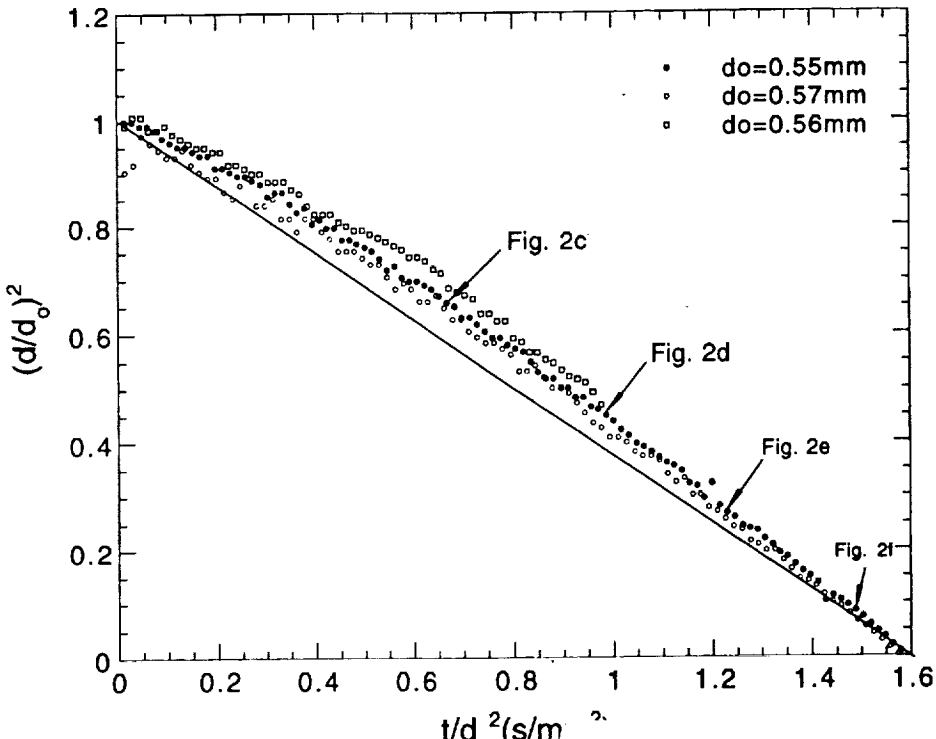


Figure